INDUSTRIAL BIPERC SOLAR CELLS WITH VARIED REAR SIDE CHARACTERISTICS UNDER BIFACIAL ILLUMINATION

N. Wöhrle[1], T. Fellmeth[1], A. Krieg[1], P. Palinginis[2], T. Weber[2], S. Steckemetz[2], K. Ramspeck[3], J. Greulich[1], S. Rein[1]
[1]Fraunhofer Institute for Solar Energy Systems ISE, Heidenhofstraße 2, 79110 Freiburg, Germany
[2]SolarWorld Industries GmbH, Am-Junger-Löwe-Schacht 2, 09599 Freiberg, Germany
[3]h.a.l.m. elektronik gmbh, Friesstraße 20, 60388 Frankfurt/Main, Germany
Telephone: +49 761 4588 5964, Fax: +49 761 4588 7621, e-mail: nico.woehrle@ise.fraunhofer.de

ABSTRACT: Bifacial solar cells pose the challenge of optimizing a solar cell's rear side towards two opposing aspects: The front side efficiency and the rear side efficiency. After a previous work of the authors has dealt with the aspects of optimizing the grid this work focusses on the passivation thickness and the rear side roughness in optical and electrical aspects. A solar cell batch with 20.6% front and 13.5% rear peak efficiency has been produced. It contains a variation of rear side capping thickness, i.e. colors, as well as planarized and textured rear surfaces which are compared under different bifacial illumination scenarios with a pure front as well as a pure rear irradiance of 1000 W/m², as well as 1000 W/m² front and added rear irradiance of 100, 300 and 500 W/m². It has been found that a textured rear surface is capable of capturing more light shining onto the rear surface, but also exhibits enhanced rear surface recombination. Under 1000 W/m² front irradiance, the threshold for rear irradiance necessary to reach parity in terms of output power between a planarized and a textured rear surface PERC is found to be between 300 and 500 W/m² on cell level using an optimal SiN_x capping thickness of 60 nm for the planar and 80 nm for the textured surface. In compound with module encapsulant the rear texture's optical trapping advantage for rear irradiated light diminishes further, increasing the required rear irradiance for output power parity above 500 W/m². The development of PERC cells with bifacialities exceeding 70% could also increase the influence of rear side optics favoring textured rear sides.
Keywords: bifacial solar cell, PERC, rear passivation, rear texture, bifaciality

1 INTRODUCTION

Bifacial PERC solar cells are still in an early stage of industrial adaption and continue to gain attraction due to their potential of a bifacial light collection [1–6]. The aim of this work is to improve the rear side collection by optimizing the surface features in terms of grid layout, surface morphology and passivation properties. After having published a simulation-optimized and verified rear side grid layout a year ago [7], which included first hints on the impact of a textured versus a planarized PERC rear side, we now want to intensify the focus on the rear side morphology and passivation.

When optimizing a bifacial solar cell's rear surface, several opposing trade-off factors have to be considered. On the optical side these are transmission of front-illuminated light through the cell's rear versus light trapping of the rear illumination into the cell. This affects the choice of metal coverage [7], surface morphology and passivation thickness. On the electrical side we have again the metal coverage [7], surface morphology (i.e. surface size) and passivation thickness (stability). By changing these factors with systematic process variations we find an optimum. Due to the bifacial character of the cells, reliable information about the results of the rear side adjustments can only be gathered with appropriate bifacial measurement. We use a current-voltage (*IV*) measurement system for solar cells with independent top and bottom light sources from h.a.l.m. elektronik GmbH offering these realistic conditions. It is described in detail in another submission [8]. By building single-cell-modules from the cell batch we follow up with an assessment of cell characteristics with the inclusion of effects of cell encapsulation for a variation of rear encapsulants.

2 EXPERIMENT

A batch of bifacial PERC solar cells on Cz p-type silicon was produced at the facilities of SolarWorld Industries yielding efficiency levels of roughly $\eta_{front} = 20.6\%$ at 1000 W/m² front and $\eta_{rear} = 13.5\%$ at 1000 W/m² rear illumination. Cells and cell precursors for characterization were provided by SolarWorld's research line and represent cell technology and performance as of 2016. The general cell parameters, except for the now varied rear side, remain the same as in Ref. [7]. This time the experiment contained two different rear side morphologies: a) A planarization by means of a chemical etch isolation and polishing process and b) a pyramid texturing process (equivalent to the

Figure 1: Visualization of the different rear cappings in a combined image (overlay) on planarized surface of the processed PERC solar cells. The SiN_x-capping thickness is (from left to right): 40, 50, 60, 80, 100 nm.

front side texture). On the rear side varying silicon nitride capping layers between 40 and 100 nm thickness have been deposited (see Figure 1). The cell batch is accompanied by characterization samples such as unmetallized precursors of each variation to determine the intrinsic open-circuit voltage (iV_{oc}) (cell area average) using the established combination [9] of photoluminescence (PL) imaging and a carrier lifetime measurement by quasi-steady-state photoconductance (QSSPC). As different trade-off mechanisms were to be expected depending on the illumination conditions, the current-voltage parameters of the produced cells were determined in a bifacial cell flasher under a combination of constant 1000 W/m² (1 sun) front irradiance and varied rear irradiance of 100, 300, and 500 W/m². The 100 W/m² rear irradiance plot is not shown in this paper to keep the length reasonable. To separate front from rear side effects, pure 1000 W/m² irradiance scenarios from front and rear side only are shown as well. Furthermore some of the cells of the optimal rear side capping thickness were incorporated into single-cell-modules to review the effects of rear side morphology on module level, which have been observed on cell level.

3 RESULTS

First of all a short overview of the results is given: Figure 2 shows the iV_{OC} results. The cell results for different illumination conditions are shown over the following pages with the *IV* parameters given in Figure 3 to Figure 6. Figure 7 finally introduces the mini-module results. All boxplots show the upper and lower quartile with the box, which is separated by the horizontal line of the median. The antennas reach to the maximum and minimum value, the arithmetic mean value is given by the open square. The little dots or diamonds give the individual sample's result. Above each boxplot the number of samples is given.

3.1 Characterization sample results

The increased recombination due to enlarged rear surface area of the pyramids on lifetime samples was accounted to $\Delta iV_{OC} = 4$ mV at the peaks, but 10-15 mV in median (see Fig. 2). Layers thinner than 100 nm show an increasing scattering indicating unstable surface passivation. While the planarized rear side shows a median loss of $\Delta iV_{OC} = 5$ mV for 60 nm thickness and $\Delta iV_{OC} = 10$ mV for 40 nm, the thin capping on textured surfaces loses large parts of its passivating property.

3.2 Cell results

Compared to planarized rear surfaces, rear side pyramids have a higher transmission loss of the front side irradiated light due to the altered angle of incidence for the light passing through a solar cell's bulk [7]. Therefore the planarized rear cells reached a peak efficiency of $\eta = 20.6\%$ ($j_{SC} = 39.3$ mA/cm²) while textured rear cells reached a peak efficiency of $\eta = 20\%$ ($j_{SC} = 39.0$ mA/cm²) for pure front irradiance of 1000 W/m² (see Figure 3). The surface enlargement loss is indicated by the pyramid rear sides being $\Delta V_{OC} = 10$-15 mV down to the planarized surfaces for all capping thicknesses between 40 and 100 nm. An additional effect is the decreasing V_{OC} for thinner capping layers, which is caused by increased surface recombination, probably due to less effective

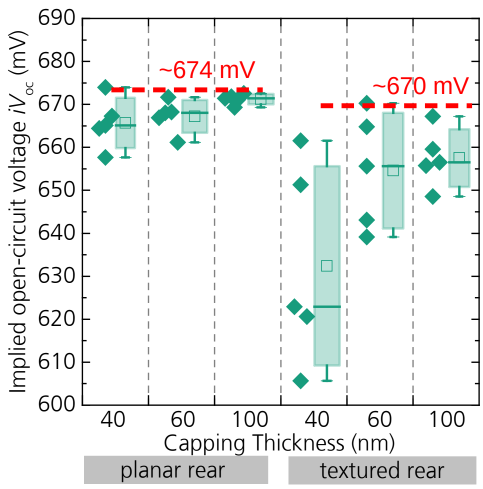

Figure 2: iV_{OC} measurements of five samples each for chosen rear layer thicknesses (40, 60, 100 nm) for planar and textured rear side. The projected upper limit for the reference thickness of 100 nm is indicated with a red dashed line.

hydrogenization and/or protection of the passivation layer by the capping layer against the rear metal. A simultaneous reduction of the fill factor is as expected observable as the maximum achievable fill factor FF_0 depends on V_{OC} [10]. Additionally it is visible that the textured rear surface has enormous spreads in passivation quality especially for reduced capping thickness. This is reflected in all three *IV* parameters indicating that a reduced passivation thickness causes problems in passivation (as already seen in the characterization samples before), optics, and capping against metal paste penetration of the passivation.

For the planarized rear surface this spread is significantly lower and capping thicknesses of 80 and 100 nm lead to a stable passivation, thicknesses down to 50 nm induce a 10% fraction of low-η cells.

To sum up, for a 1000 W/m² front illumination the planarized rear cells have a peak advantage of $\Delta\eta = 0.6\%$, moreover the textured rear side is susceptible towards unstable passivation if its SiN_x-capping thickness is reduced below 100 nm.

For pure rear side illumination of 1000 W/m² (Figure 4) a significant additional factor joins the equation: Rear light trapping. While it is obvious for pure rear illumination it plays a crucial role in bifacial illumination. The rear texture improves the light trapping of rear irradiated light, hence antagonizes the mentioned disadvantages of a textured rear against a planarized surface.

For the pure rear illumination (Figure 4) this leads to an optical advantage of $\Delta j_{SC} \approx 2$ mA/cm² for an optimal rear capping thickness of 60-80 nm. Despite the still reduced V_{OC} (5-10 mV less) this leads to an advantage for the textured rear over the planarized rear with $\eta_{text} = 13.5\%$ and $\eta_{planar} = 12.6\%$. Nevertheless the strong fluctuation inside the groups prevails. This means we have to assume that with process adjustments it is possible to produce a more solid capping layer with more consistent passivation results.

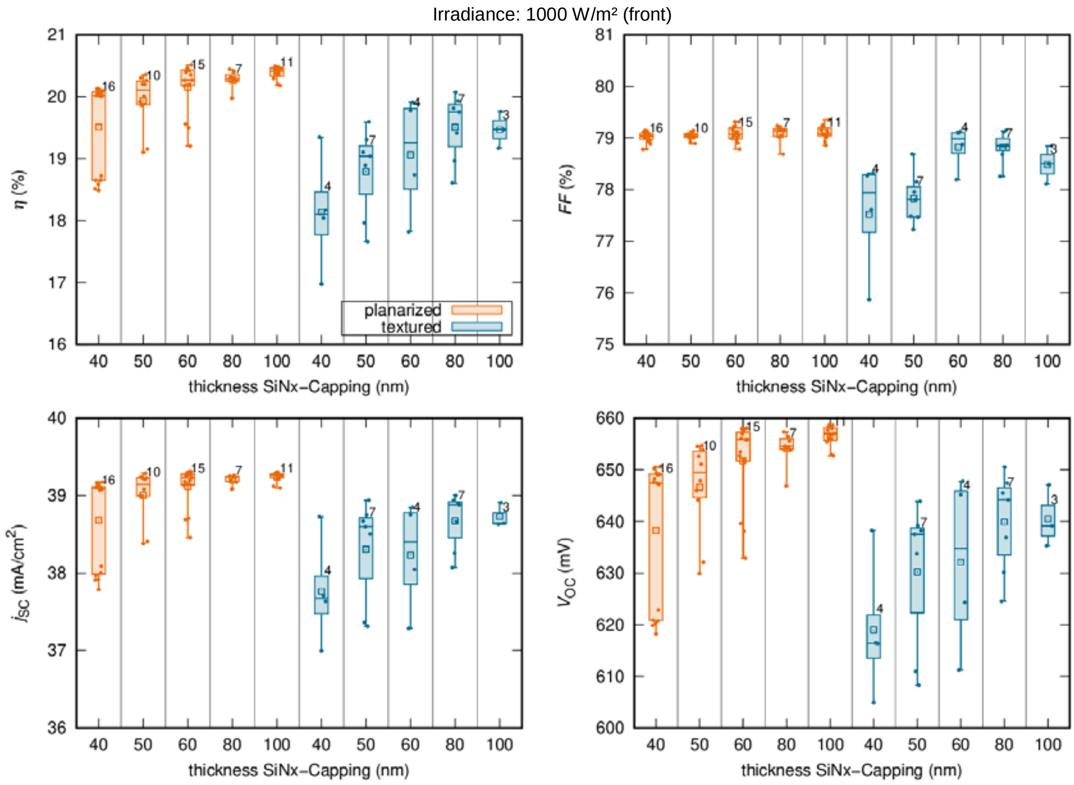

Figure 3: Measured front *IV* parameters for the biPERC cells with varied rear capping (SiN_x) thickness from 40 to 100 nm. The orange box plots show the results on chemically planarized rear, the blue boxes on random pyramid textured rear. The pure front illumination shows the optical advantage for the planarized rear side in short-circuit current by $\Delta j_{SC} \approx 0.5$ mA/cm² mainly due to less transmitted light. The scattered values, especially with the textured rear have their origin in rear surface recombination. The loss in open-circuit voltage ΔV_{OC} is approximately 10 mV for the textured rear surface against the respective planarized counterpart, if outliers are ignored. This is mainly caused by enhanced rear surface recombination.

The relevant follow-up question is if there's a relevant illumination scenario where a cell with textured rear side can overcompensate the deficits it has at front side illumination with rear side collection gains.

The flipping point for optical advantage in the simulation in the previous work [7] was determined to be at 300 W/m² rear irradiance additionally to the 1000 W/m² front irradiance. The bifacial measurements of our cells (Figure 5, Figure 6) show the break-even rather between 300 and 500 W/m² for an optimized capping thickness of 60-80 nm. As presumed this equality for the textured rear against the planarized rear cell is achieved by a balance of a superior optics (higher j_{SC}) and inferior passivation quality and stability (lower V_{OC} & *FF)*. This also implies a consistent deposition process avoiding the strong fluctuations we still see. In a scenario where the rear irradiation surpasses the 300 W/m², Figure 6 displays measured 1000 + 500 W/m² bifacial irradiance, the balance finally flips towards an advantage (however a small one) for the peak of the textured rear cell, again driven by gains in j_{SC}.

3.4 Mini module results

For the mini modules the results for 1000 W/m² front and for 1000 W/m² rear illumination are shown in Figure 7. The plots start with the selected cell results, which then have been encapsuled in modules with different types of backsheets (glass, transparent foil, white foil) to provide different optics. The orange boxes represent planarized rear, the blue boxes textured rear surface. The cells all feature 80 nm rear capping thickness.

Unfortunately the glass-glass module assembly suffered from a contacting issue so its *FF* results are hard to compare with the other module results. Nevertheless it is visible that for front irradiation the rear side sheet type (transparent vs. white) makes no significant difference in cell efficiency and the loss on cell level from the textured rear against the planarized rear cell is directly reflected in module compound, both yielding $\Delta\eta \approx 0.5\%$.

For the case of 1000 W/m² rear illumination however the picture is more differentiated. The planarized rear cells have j_{SC} = 24 mA/cm² both on cell and module level (with glass as well as transparent backsheet). The textured rear cell's superior current of j_{SC} = 26.8 mA/cm² diminishes to 26.2 mA/cm² with a glass encapsulant and to 25.5 mA/cm² with a sole transparent backsheet. This kind of effect is known [11] and can be explained by external light reflection at the air-glass or air-backsheet interface and light trapping within the module, i.e. internal reflection.

As a result the advantage of the improved rear collection of the textured rear side is generally weakened in module encapsulation. The found flipping point at 1000 + 500 W/m² on cell level will thus not be sufficient on module level. Since the advantage on cell level is still small at 1000 + 500 W/m², this can be considered as a minimum rear irradiation for a bifacial cell with textured rear showing higher output power on module level.

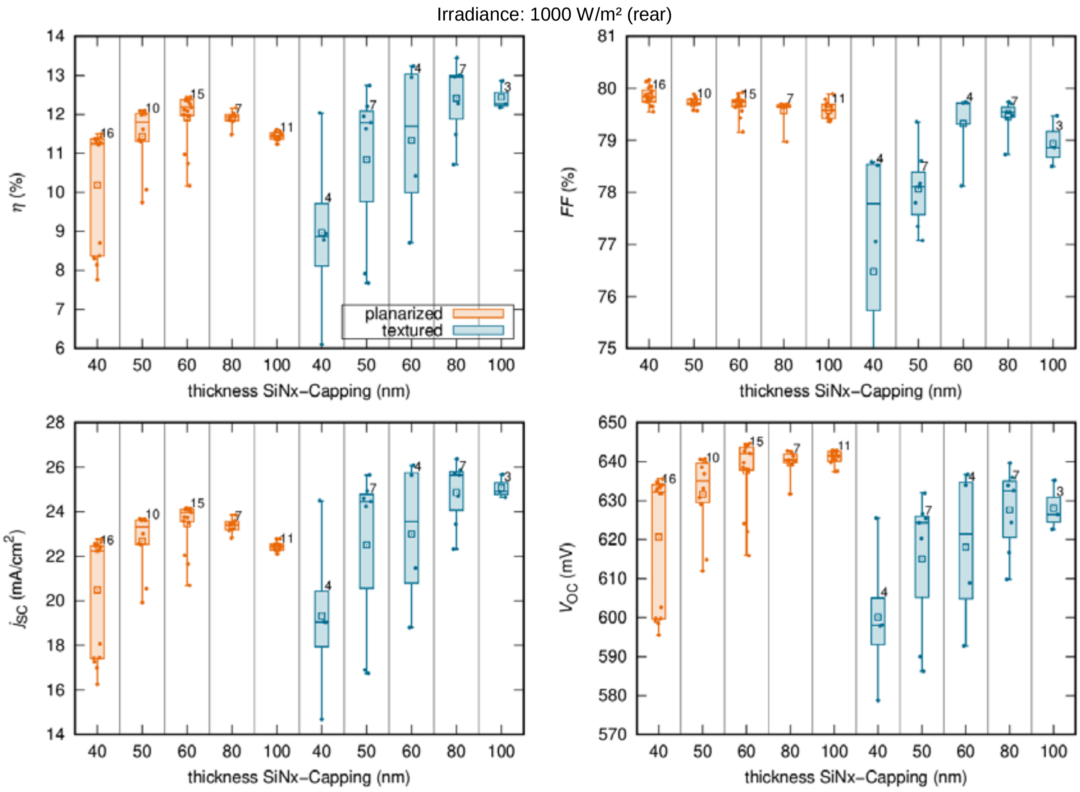

Figure 4: Measured rear *IV* parameters for the biPERC cells at 1000 W/m² rear illumination with varied rear capping (SiN_x) thickness from 40 to 100 nm. The orange boxplots show the results on chemically planarized rear, the blue boxes on random pyramid textured rear. The pure rear illumination shows the optical advantage of the textured surface of $\Delta j_{SC} \approx 2.8$ mA/cm² due to improved light trapping. V_{OC} is still in disadvantage by 10 mV, yielding a remaining efficiency advantage of $\Delta\eta \approx 1\%$. The optimum capping thickness is at 60 nm for planar and 80 nm for textured rear sides.

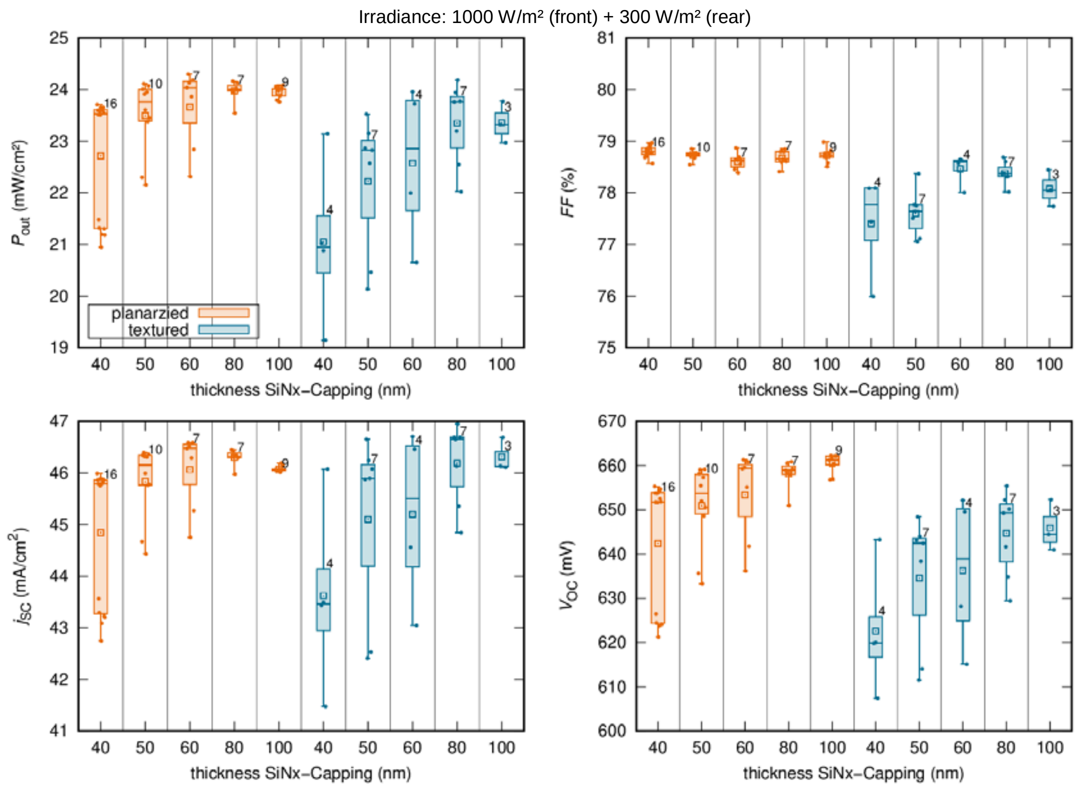

Figure 5: Measured *IV* parameters for the biPERC cells with varied rear capping (SiN_x) thickness from 40 to 100 nm for bifacial irradiance of 1000 W/m² (front) + 300 W/m² (rear). The orange boxes show the results on chemically planarized rear surface, the blue boxes on random pyramid textured rear. With this irradiance the improved light trapping of the textured rear compensates the losses by transmission of front irradiated light (compare maximum j_{SC} of the blue group against the orange group). However the higher recombination loss of the textured rear (*FF* and V_{OC}) still slightly discriminates the texture against the planarized rear in maximum output power (at 60 and 80 nm thickness) with 24.4 against 24.1 mW/cm².

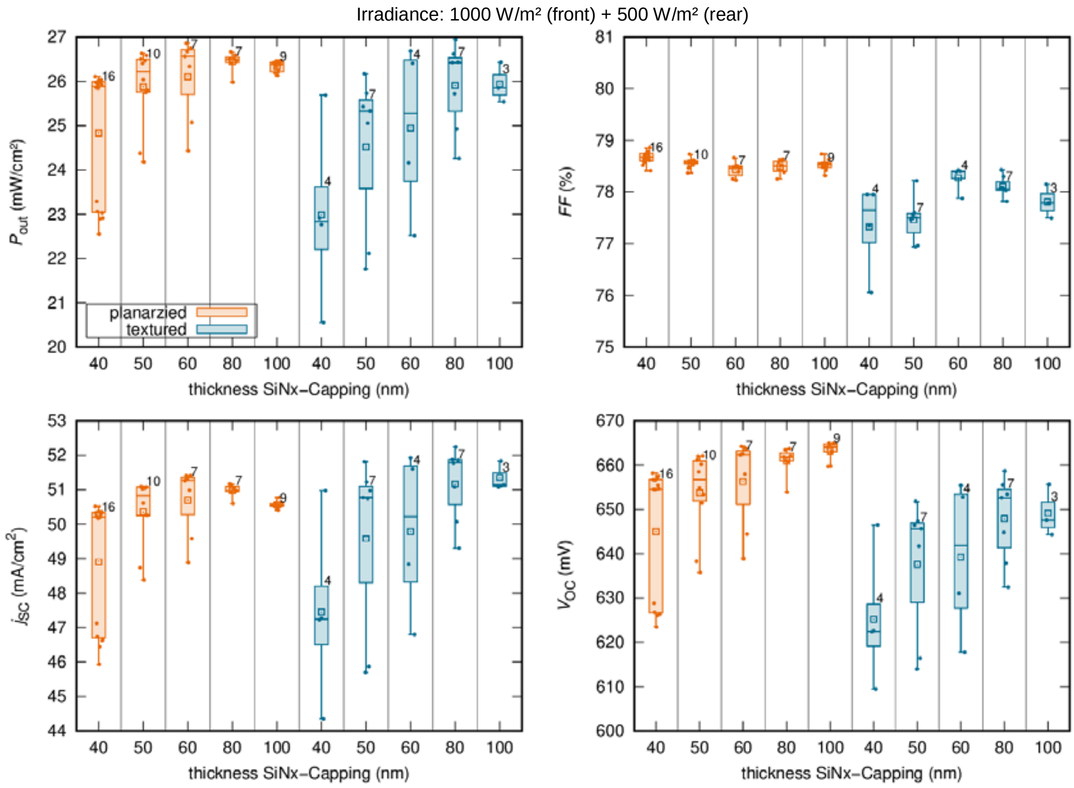

Figure 6: For 1000 W/m² (front) + 500 W/m² (rear) irradiance the improved light trapping of the texturized rear side yields 1 mA/cm² increased maximum j_{SC} over the planarized surface. This compensates the recombination losses and the planarized and texturized rear yield the same maximum p_{out} = 27 mW/cm² for the ideal rear capping thickness of 60 and 80 nm. However the efficiency scattering of the groups, especially the texturized rear sides imposes the need for cautious observation of the capping stability and a process tuning for the deposition step. Further an improvement in process stability for thinner layers would also reduce the general disadvantage of the textured rear in *FF* and V_{OC}, as the recombination beneath the rear fingers could be confined. In effect the textured-rear cell might reach rear parity to the planarized-rear cell at lower rear irradiance than 500 W/m².

4 DISCUSSION AND CONCLUSION

For our solar cell setup we conclude that a textured rear side on bifacial PERC solar cells can unfold its rear light trapping advantage only at comparably high rear irradiances of 500 W/m² or higher (in combination with a simultaneous front irradiance of 1000 W/m²). This exceeds most application scenarios with front illumination and rear albedo. It also exceeds the values discussed for a draft of a bifacial measurement norm of the IEC 60904-1-2, which currently considers 100 or 200 W/m² additional rear irradiance.

Furthermore, the optimization of the rear capping thickness follows the same rules as on the front side (if the expected spectrum is similar to AM1.5G) thus leading to 60 nm SiN_x-capping-optimum in our case (due to a second thin passivation layer beneath). However this is heavily influenced by the stability of the passivation, which tends to degrade for thicknesses lower than 80 nm, especially for textured or rough surfaces. Therefore, if no exceptionally high rear irradiance is expected, a conventional planarized rear side with a dark blue anti-reflection capping is the optimal solution for bifacial PERC cells and modules yielding the highest overall power output. This has been shown by our simulations [7] and the present experiment.

These findings are however limited to cell configurations with sufficient similarity to the solar cells we used. A bifaciality (ratio of rear and front efficiency) around 60% is rather low by today’s standards. Industrially feasible PERC studies with bifacialities of 70-90% have been shown [5, 7, 12] giving the rear side optics a higher significance and which again lowers the threshold for rear the irradiance necessary favoring textured rear sides.

Furthermore alternative illumination scenarios are thinkable which might also shift the balance towards a textured rear side. In particular these can be weak light scenarios for the front side with less than 1000 W/m² irradiance such as vertical panel installations.

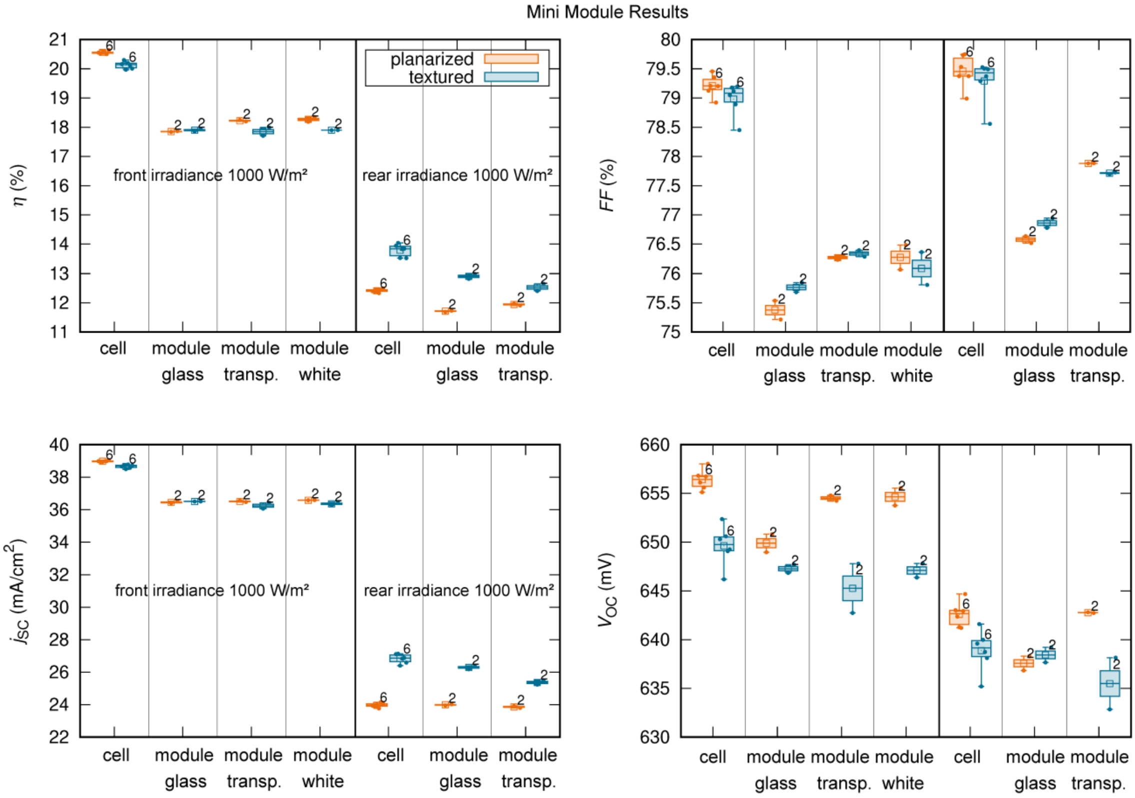

Figure 7: Mini module results for cells with 80 nm rear capping thickness each. The *IV* plots each show the cell results first, followed by the same cells built into 1-cell-mini modules with a glass rear encapsulation, a transparent backsheet or a white backsheet. The columns for rear side illumination lack the white backsheet for obvious reasons. The orange boxes show the cells with planarized rear side, the blue boxes show the textured rear side.

ACKNOWLEDGEMENTS

This work was conducted within the project "BiZePS" (FKZ: 0325909), supported by the German Ministry for Economic Affairs and Energy.

We thank .h.a.l.m elektrinik and SolarWorld Industries for the fruitful cooperation and wish all SolarWorld employees the very best for their future.

REFERENCES

[1] J. Parnell, *Intersolar Europe: SolarWorld to launch glass-glass bifacial modules.* [Online] Available: https://www.pv-tech.org/news/intersolar_europe_solarworld_to_launch_glass_glass_bifacial_modules. Accessed on: Mar. 09 2018.

[2] T. Dullweber *et al.*, "PERC+: Industrial PERC solar cells with rear Al grid enabling bifaciality and reduced Al paste consumption," *Prog. Photovolt: Res. Appl.*, vol. 24, no. 12, pp. 1487–1498, 2016.

[3] R. Kopecek and J. Libal, "Bifaciality: still an advantage for n-type?," Freiburg, 2017.

[4] K. Krauß, F. Fertig, J. Greulich, S. Rein, and R. Preu, "biPERC silicon solar cells enabling bifacial applications for industrial solar cells with passivated rear sides," *Phys. Stat. Sol. (a)*, vol. 213, no. 1, pp. 68–71, 2016.

[5] E. Lohmüller *et al.*, "Bifacial p-type PERL solar cells with screen-printed pure Ag metallization and 89% bifaciality," in *33rd EU PVSEC*, Amsterdam, The Netherlands, 2017.

[6] T. Fellmeth *et al.*, "Co-diffused bi-facial PERT solar cells," *Energy Procedia*, vol. 124, pp. 875–880, 2017.

[7] N. Wöhrle *et al.*, "Understanding the Rear-Side Layout of p-Doped Bifacial PERC Solar Cells with Simulation Driven Experiments," *Energy Procedia*, vol. 124C, pp. 225–234, 2017.

[8] A. Krieg *et al.*, "IV-measurements of bifacial solar cells in an inline solar simulator with double-side illu-mination," in *35th EU PVSEC*, Brussels, submitted, 2018.

[9] B. Hallam, B. Tjahjono, T. Trupke, and S. Wenham, "Photoluminescence imaging for determining the spatially resolved implied open circuit voltage of silicon solar cells," *J Appl Phys*, vol. 115, no. 4, p. 44901, 2014.

[10] M. A. Green, "Accuracy of analytical expressions for solar cell fill factors," *Solar Cells*, vol. 7, no. 3, pp. 337–340, 1982.

[11] J. Greulich *et al.*, "Optical simulation and analysis of iso-textured silicon solar cells and modules including light trapping," *Energy Procedia*, vol. 77, pp. 69–74, 2015.

[12] T. Dullweber *et al.*, "Present status and future perspectives of bifacial PERC+ solar cells and modules," *Jpn. J. Appl. Phys.*, vol. 57, no. 8S3, 08RA01, 2018.